Evaluating LTE Coverage and Quality from an Unmanned Aircraft System

Michael Nekrasov, Vivek Adarsh, Udit Paul, Esther Showalter, Ellen Zegura*,
Morgan Vigil-Hayes† and Elizabeth Belding
UC Santa Barbara, {mnekrasov, vivek, u_paul, ehs, ebelding}@cs.ucsb.edu
*Georgia Tech, ewz@cc.gatech.edu
†Northern Arizona University, morgan.vigil-hayes@nau.edu

***Abstract*—Despite widespread LTE adoption and dependence, rural areas lag behind in coverage availability and quality. In the United States, while the Federal Communications Commission (FCC), which regulates mobile broadband, reports increases in LTE availability, the most recent FCC Broadband Report was criticized for overstating coverage. Physical assessments of cellular coverage and quality are essential for evaluating actual user experience. However, measurement campaigns can be resource, time, and labor intensive; more scalable measurement strategies are urgently needed. In this work, we first present several measurement solutions to capture LTE signal strength measurements, and we compare their accuracy. Our findings reveal that simple, lightweight spectrum sensing devices have comparable accuracy to expensive solutions and can estimate quality within one gradation of accuracy when compared to user equipment. We then show that these devices can be mounted on Unmanned Aircraft Systems (UAS) to more rapidly and easily measure coverage across wider geographic regions. Our results show that the low-cost aerial measurement techniques have 72% accuracy relative to the ground readings of user equipment, and fall within one quality gradation 98% of the time.**

***Keywords*-LTE, Aerial Networks, Mobile Broadband, Software Defined Radios, Cellular Coverage, RSRP, UAS.**

I. Introduction

Billions of users worldwide benefit from high-speed internet access provided by LTE. However, economic incentives often drive LTE and other broadband technology expansion, concentrating deployment in populated urban areas. Economically marginalized and sparsely populated rural areas remain underserved [1]. In the United States, for example, rural tribal regions suffer from the poorest LTE coverage [2]. Even when cellular providers claim coverage, poor signal quality can limit achievable download data rates far below the mobile broadband threshold, defined by the U.S. Federal Communications Commission (FCC) as a median speed of 10 Mbps [2].

For underserved regions in the United States, the FCC has instituted incentive programs to offset provider infrastructure deployment costs [3], [4]. These programs first determine the bounds of existing coverage and identify coverage deficiencies by semi-annually collecting network connectivity reports from commercial network operators. Every operator that owns cellular network facilities in the United States participates in data collection by submitting a Form 477 [5]. The reported coverage area consists of geo-polygons using operator-defined methodology. Based on this data, the FCC allocates subsidies to incentivize commercial coverage in underserved regions and verifies compliance.

The FCC publicly releases annual Broadband Deployment Reports (e.g. [2]), as well as shapefiles for each operator that indicate geographic coverage areas [5]. However, researchers challenge their accuracy [6]–[8]; for example, Meinrath et al. examined a public dataset of speed tests collected by the Measurement Lab [9], [10] and demonstrated that broadband access in Pennsylvania is much lower than claimed in the report. This inaccurate over-reporting can be attributed to the proprietary and often generous propagation models used by network operators [11]. To validate the true state of mobile broadband access, we need publicly controlled methods for measuring coverage areas and signal quality, particularly in regions typically underserved.

To audit provider-reported coverage claims, third parties undertake independent measurement efforts. While the concept of "coverage" remains imprecise [12], network parameters such as the received signal strength (in terms of Reference Signal Received Power (RSRP)) are typically used to estimate the extent of network availability. Popular public crowdsourcing platforms, such as CellMapper [13] or OpenSignal [14], collect measurements from network users and calculate cellular coverage and signal quality. Data from crowdsourced efforts provide information over time and for a wide range of devices, but these data cluster around major transportation arteries, omitting communities outside of these areas. An alternative collection strategy employs specialized equipment with dedicated users. For example, wardriving typically involves physically navigating difficult terrain in remote areas to record on-the-ground measurements [15]. This method enables greater control over the measurement process and the geographic scope but scales poorly due to considerable time investment and labor costs.

Because existing strategies suffer from the aforementioned drawbacks, we need alternative solutions for measuring LTE coverage and signal quality. An ideal strategy should enable quick assessment using measurements of the RF landscape throughout large areas (on the order of square miles), even if hard-to-access. In addition, new strategies should provide scalability with respect to equipment and human resources.

Based on these criteria, off-the-shelf software defined radios offer a viable solution. However, because SDRs can cost anywhere between tens of dollars to a few thousand dollars, it is important to study the relationship between precision of readings and the cost of the equipment, to determine whether more affordable equipment will suffice.

To reduce human effort of spectrum scans, Unmanned Aircraft Systems (UAS) can carry payloads while maintaining appreciable flight times. The availability of low cost, programmable, highly agile unmanned aerial vehicles has spurred interest in employing aerial RF sensing for cellular coverage mapping [16], [17]. UASs enable coverage for large geographic areas, which may be costly, difficult, or impossible to cover on foot or in land vehicles. Network operators, such as Verizon, already employ UASs for visually inspecting equipment after natural disasters [18]. Extending UAS capabilities to include signal measurements is an active area of interest for a variety of wireless applications [19], [20]. These extensions could further enable uses for scalable rural cellular coverage mapping as well as post-disaster recovery efforts. Small form-factor Software Defined Radios (SDR) with high sensitivity, such as the RTL-SDR (RTL2832U chipset with a Elonics E4000 Tuner), are proving increasingly useful for LTE applications [21]–[23]. This SDR is perfectly suited for UAS application. However, the high altitude of UAS flight, relative to the ground, poses challenges to the efficacy of these approaches. As antennas on LTE towers are provisioned for ground transmission, the RF radiation pattern picked up at high altitudes may not reflect signal quality on the ground [24].

In this paper, we assess the accuracy of a low-cost, small form-factor RTL-SDR for sensing LTE eNodeB signal strength over a wide area through integration with an off-the-shelf quad-copter UAS. To do so, we first compare reading accuracy of this airborne sensor with commonly used hardware for ground-based wardriving approaches (i.e a spectrum analyzer and a USRP). Further, because no existing studies systematically examine the effect of altitude on signal strength measurements, we fly the UAS at varying altitudes across multiple locations and examine how aerial signal sensing can be aligned to ground-level measures. Because minimal previous research compares observed signal strength between measurements collected by user equipment (UEs) (i.e smartphones, tablets, and hotspots) and UASs, we deployed four cellular devices on the ground, each collecting measurements from different cellular networks, and compared these measurements over the same geographic area to those collected by the RTL-SDR on the UAS. We look to the UE measurements as "ground truth" because the UE readings capture examples of the actual coverage and performance a user, in the given location, would experience with UE.

Our findings reveal that the simple RTL-SDR has comparable accuracy to expensive solutions and can estimate quality within one gradation of accuracy when compared to user equipment. Further, we show that these devices can be mounted on a UAS to more rapidly measure coverage across wider geographic regions. Our results show that the low-cost aerial measurement techniques have 72% accuracy relative to the ground readings of user equipment, and fall within one quality gradation 98% of the time. Our findings, taken together, offer a detailed look at the efficacy of low-cost, public controlled, aerial coverage and quality sensing.

This paper proceeds as follows: Section II overviews related work. Section III explains the methodology and the corresponding datasets, while our analysis and results are presented in Section IV. Section V discusses impact of this study and future work, and Section VI concludes the paper.

II. Related Work

RF Spectrum Sensing with SDRs: Previous studies involving wide-scale cellular sensing include analysis of GSM pollution [25] and propagation model verification for LTE signals [26]. In one study, an SDR was mounted on a UAS to navigate the flight path by LTE location signalling [27]. In contrast, our study uses only passive sensing with a very lightweight SDR to discover ground truth signal strength readings. We show that low-cost equipment detects LTE availability to produce a coverage map, using RSRP measurements, that aligns with the ground truth UE measurements. In our study, we adapt a wide-scale television white space sensing approach used by Saeed et al. [28], but we adjust for LTE instead of TV frequencies.

RF Spectrum Sensing with UASs: Considerable prior work has focused on identifying the application of UASs for cellular networks. Batistatos et al. [16] study the variation in LTE signal strength and SINR for both an underserved rural area and an urban center. A UAS connected to an existing LTE network monitored the LTE signals in a range of different altitudes [17]. The authors found that at 60m to 100m above the ground, LTE coverage probability climbs to 90% and the received power gains 18 dB with respect to the ground level. This work, however, did not compare measurements taken from the aerial platform to measurements taken from a ground-level UE.

Lin et al. [24] shed light on the applicability and performance of mobile network connectivity to low altitude UASs by analyzing downlink channel indicators, such as RSRP. While the study in [29] examines the variation of RSRP, RSRQ, and SNR throughout a drive-by style campaign in an urban university campus using a passive monitoring device, little prior work has explored the effective measurement of received signal strength using SDRs accompanied by an adequate validation from UE readings.

LTE Performance Measurement with RSRP:

Estimation of received signal strength plays a vital role in many control plane operations, including inter- and intra-eNodeB handovers [30]–[34]. Precise detection of RSRP plays a crucial role in these handovers, as well as several diagnostic methods in LTE networks. For instance, Anas et al. [35] evaluate the performance of RSRP handovers in LTE. They observe that a handover margin of 2dB to 6dB (RSRP) leads to an optimal number of handovers without sacrificing much of uplink SINR (for a specific range of user velocity). The

effect of RSRP measurement bandwidth on the accuracy of handovers is studied in [34], [36]. From a telecom provider's perspective, this suggests a need for up-to-date, accurate RSRP space-maps for improving service quality.

Several prior works examine the relationships between RSRP, RSRQ and SINR [37]–[40], but little work explores the correlation between passive monitoring of LTE channels and ground UE readings. In [41], the researchers examine the viability of deploying LTE connectivity using UASs in a rural area. Their results indicate that the coverage outage level increases from 4.2% at an altitude of 1.5 m to 51.7% at 120 m under full load conditions. Another study analyzed a set of live network measurements conducted with an LTE scanner attached to an airborne UAV [42]. The findings suggest improved radio clearance as the UAV increases altitude. The increase in the average number of detected cells, as altitude increases, corroborates these findings. To the best of our knowledge, our study offers the first look into conducting reliable RSRP measurements with UAS using low-cost off-the-shelf SDRs.

III. System Overview and Methodology

We collected ground and air measurements in two regions in Rio Arriba county, New Mexico over a period of five days, beginning May 28, 2019. For each region, we obtained permission to drive through residential areas, as well as to fly a UAS equipped with a sensor.

In this section, we describe the six unique RF sensing methodologies employed in our analysis. Like all wardriving studies, our work is necessarily limited in scale. However, these ground measurements are uniquely useful for contrasting the efficacy of each measurement technique. In all cases, our methodology is generalizable. Figure 1 shows images of many of our sensing set-ups.

A. Method 1: Ground-Driven User Equipment (UE) Sensing

In our wardriving campaign, we record signal strength readings from four Motorola G7 Power (XT1955-5) phones, each running Android Pie (9.0.0). We collect measurements using the Network Monitor application [43]. An external GlobalSat BU-353-S4 GPS connected to an Ubuntu Lenovo ThinkPad laptop gathered geolocation measurements, which we matched to the appropriate ground measurement by timestamp. We outfitted each phone with a SIM card from one of the four top cellular providers in the region: Verizon, T-Mobile, AT&T, and Sprint. The phones recorded signal strength every 10 seconds while we drove at speeds less than 10 miles per hour through the areas of study.

B. Method 2: Ground-Driven Spectrum Analyzer

We gathered measurements on LTE channel center frequencies with a high-precision Keysight N9340b spectrum analyzer (SA) using a ham radio antenna capable of sensing signals up to 3 GHz. The SA was transported inside the measurement vehicle while the antenna was magnetically mounted to the roof.

(a) UE (b) Ground Measurement Kit

(c) UAS (d) Stationary box.

Fig. 1: Sensing Equipment.

C. Method 3: Ground-Driven USRP

We collected center frequency readings with a Ettus Research USRP B200, a versatile software defined radio widely used for LTE and TV frequency experimentation and sensing. The USRP measured the same set of LTE channel center frequencies as the SA through a ham radio antenna placed beside the identical SA antenna.

D. Method 4: Ground-Driven RTL-SDR

We also collected center frequency readings with a NooElec RTL-SDR RTL2832U and Elonics E4000 Tuner, an inexpensive software defined radio operating in the 55MHz-1100MHz and 1500MHz-2300MHz ranges. The RTL measured LTE channel center frequencies through a ham radio antenna placed beside the identical SA and USRP antennas.

Unlike the USRP B200, which when inside a transportable case is bulkier and more expensive, the RTL-SDR is low-cost and protected in a smaller form-factor. This specific model of RTL-SDR covers most LTE frequencies and is simple to equip onto a UAS or deploy at a stationary site for long-term monitoring. This ground-transported RTL-SDR serves as a comparison point for the UAS and longitudinal sensing experiments described subsequent subsections.

E. Methods 5: Aerial Sensing Platform

Our UAS consisted of a DJI Matrice 100 quad-copter, as shown in Figure 1c. The UAS collected signal strength readings via a NooElec RTL-SDR (the same model as used for ground measurements) connected to a Raspberry Pi 2—Model B on-board computer via USB. The location of the UAS was

recorded from the Matrice 100 on-board GPS, sampling at a rate of 50 Hz and using a UART connection to the Pi.

1) Horizontal Coverage Mapping: In one set of experiments, we flew the UAS manually at varying speed and elevation (in order to clear obstacles and keep the UAS in line of sight) to map coverage. We attempted to cover the same areas as covered by the UE and ground measurements. For each geographic area, UAS measurements occurred on the same day as the other data collection, but sometimes several hours apart.

2) Vertical Experiments: To investigate the impact of elevation on signal strength measurements, we performed four sets of vertical-only flights. Each set of flights was conducted in a different geographic region of our measurement area. During each vertical flight, the UAS was raised by 10ft increments approximately every 15 seconds to 100ft. It was then raised in 20ft increments approximately every 15 seconds to 400ft (the maximum FAA non-exempt altitude limit).

F. Method 6: Stationary Box

Because continuous monitoring in an area can be costly in terms of equipment and manpower, coverage mapping is typically completed via sampling over a short time-frame. For example, in our ground sensing driving campaign, we take all samples over a maximum of one hour for each unique location. As part of our study, we seek to verify that this one-shot sensing method is appropriate for estimating long-term spectrum availability.

We therefore measure spectrum occupation over time in a single location to monitor changes. We enclosed a NooElec RTL-SDR (the same model as is utilized by the ground measurements and UAS) run by a Raspberry Pi 3 B+ in a weather-proof case with the stock antenna on top the case, shown in Figure 1d. Over two days, the RTL continuously iterated through a pre-programmed list of all 20 known LTE frequencies for the four network providers in the area and recorded signal strength readings for each frequency every three seconds.

This method monitors the stability of the RTL-SDR measurements over time and can indicate the appropriate flight time necessary to generate a consistent measure of signal quality in an area. While this data is not generalizable geographically, it provides insight into the precision of signal strength reading from an RTL-SDR.

G. LTE Channel Selection by Provider

Before data collection, we compiled a list of LTE cellular frequencies in use by the top providers in the area. This was needed for every sensing method other than the UEs, which pulled the active frequencies automatically for their respective provider. We compiled this list using two complementary processes. First, on each UE we ran CellMapper [13], an Android application that allowed us to query the active frequencies detected by the device for the corresponding LTE provider. We supplemented this list with a scan using a spare Ettus Research USRP B200, equipped with a wideband LTE dipole antenna [44], connected to a Lenovo ThinkPad laptop running srsLTE [45]. Using srsLTE we performed a scan of all possible LTE frequencies operated in the United States and appended to our list any frequencies not previously discovered. Since UEs choose the strongest frequency to communicate with a nearby base station, this allowed us to locate other frequencies available from nearby cells which the UEs would not use at our test sites but could jump to intermittently. As we moved between regions, we added all newly detected frequencies to the list scanned by all sensors.

	UE	**UAS**	**Spectrum Analyzer**	**USRP**	**RTL-SDR**
UE	1152	-	-	-	-
UAS	305	812	-	-	-
Spectrum Analyzer	131	53	1199	-	-
USRP	131	53	1199	1199	-
RTL-SDR	131	53	1199	1199	1199

TABLE I: Number of overlapping geographic bins by signal collection method.

The resulting list contained 22 frequencies in operation in the area, served by the four providers. Because the NooElec RTL-SDR is limited to a frequency of 2300 MHz, two of the detected frequencies (2628.8 MHz and 2648.6 MHz) were outside the range frequencies we could sense on the Ground RTL, Stationary Box, or UAS and are dropped from our analysis.

IV. Analysis

A. Accuracy of Data Collection Methods

1) Preparing data for geographical analysis: Because multiple devices and personnel participated in data collection, the data was not sampled at the same exact timestamp or precise GPS location for all methods. For example, both the ground sensors and the UAS passed over the same residential area but may not have covered the same 1 meter GPS coordinate due to road availability. To accurately compare data collected by different methods, we first aggregate data into geographical bins of three decimal places of GPS accuracy, approximately 110 square meters in area. Then, for each method and for each set of readings on different LTE frequencies, we take the mean across all the signal strength values that fall into that geographic bin.

The data collected by the UEs included only the network provider (AT&T, Sprint, T-Mobile, and Verizon), and not the frequency on which the UE was operating. To compare this to the other data collection methods, which report frequency instead of network, we first map each frequency to the corresponding network provider using the frequency list we describe in Section III-G. For each network provider and geographic bin, we then select the frequency with the strongest signal strength and set that as the signal strength for the provider in that bin. This method resulted in 2,637 unique 110m^2 geographic bins. Not every area was sampled by every method. The resulting overlap between methods and geographic area is summarized in Table I.

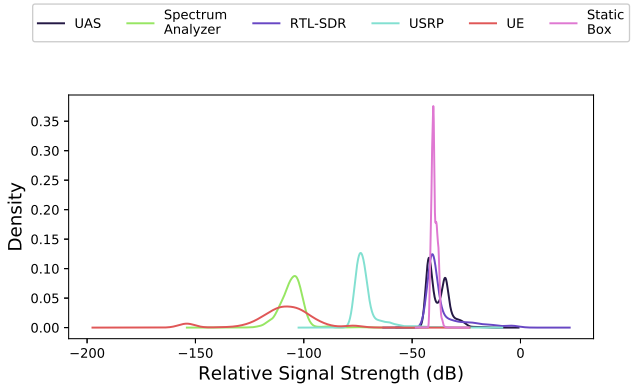

Fig. 2: Kernel density estimation of original data by signal collection method.

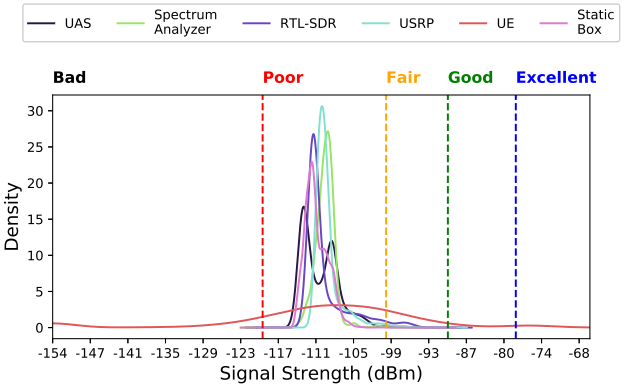

Fig. 3: Kernel density estimation of transformed distributions by signal collection method.

2) Transforming Raw Signal Readings: The UEs, spectrum analyzer, RTL-SDR modules (including both the one mounted on the UAS and in the stationary monitoring box), and the USRP all report signal strengths on varying scales. We show the original distribution of the relative signal strengths for each collection method in Figure 2. As we can see, while the distributions have similar normal-like peaks, the offsets and width of the distributions do not match.

While the spectrum analyzer outputs dBm, the other devices report relative signal strengths. As we are interested in the experience of the end user, before comparing data collection methods, we first need to transform the raw relative signal strength readings to match the UEs.

To do so, we first perform a min/max normalization on each method, as shown in Equation 1, where $\vec{O}$ is the original data, $m \in \{$*spectrum analyzer, USRP, RTL, UAS*$\}$ is the method and $\vec{N}$ is the normalized data.

$$\vec{N}_m = \frac{\vec{O}_m - \min(\vec{O}_m)}{\max(\vec{O}_m) - \min(\vec{O}_m)} \tag{1}$$

Next we offset and scale the other methods to align them with the signals received by the UE. To do this we randomly selected 50% of our data as a training set. On this training set for each method we find an offset x_m and scaling factor a_m to minimize Equation 2, where n_m and n_{ue} are measures taken from the same geographic bin and cellular network provider. If a method does not have a matching UE measurement, it is omitted from the sum.

$$\min_{x_m, a_m} \left(\sum_{n_m \in \vec{N}_m} [a_m(n_m + x_m) - n_{ue}]^2 \right) \tag{2}$$

Finally we scale and offset *all of our data* for every method other than the UE by x_m and a_m, and scale back to the readings of the UE as expressed in Equation 3, where $\vec{T}_m$ is the resulting transformed data for each method.

$$\vec{T}_m = \left[a_m\left(\vec{N}_m + x_m\right)\right]\left(\max(\vec{N_{ue}}) - \min(\vec{N_{ue}}) + \min(\vec{N_{ue}})\right) \tag{3}$$

By transforming the data we can now compare signal strength readings to one another and to the UE. The resulting transformed distributions are shown in Figure 3. For the rest of our analysis, we use this transformation when we report signal strength values in dBm.

3) Estimating signal strength: We computed the Pearson correlation on each method pair and found only a weak linear relationship between the collection methods and the readings from the UEs, even after transforming the data. As signal strength can vary, even between different UE device makes and models, we categorize the level of signal quality rather than predicting the exact signal strength a UE would receive in an area by dividing the signal strength levels into five groups, based on criteria in Table II. While there is no standard for defining what LTE signal strength corresponds to what quality, we model our criteria after those suggested by SignalBooster [46].

Based on this categorization we compare how each method sorted the signal strength readings across the geographical bins, using the UE as ground truth. We summarize our results in Figure 4. The UAS was most closely aligned with the UE, matching values exactly for 72% of the geographic bins. When allowing for one signal quality of discrepancy (for instance,

Signal Quality	Range	Color
Bad	<120 dBm	Black
Poor	-120 to -111 dBm	Red
Fair	-111 to -105 dBm	Orange
Good	-105 to -90 dBm	Green
Excellent	>90 dBm	Blue

TABLE II: Categorization of signal strength into signal quality bins.

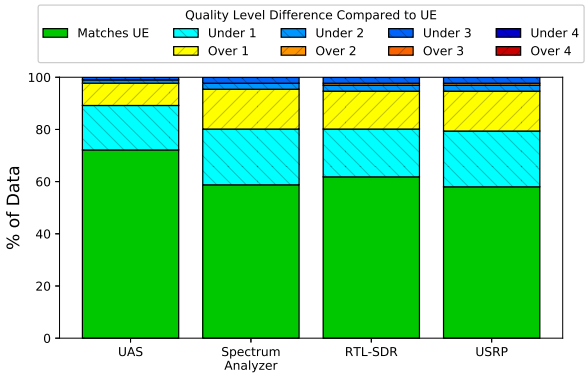

Fig. 4: Accuracy of signal collection methods as compared to the UEs.

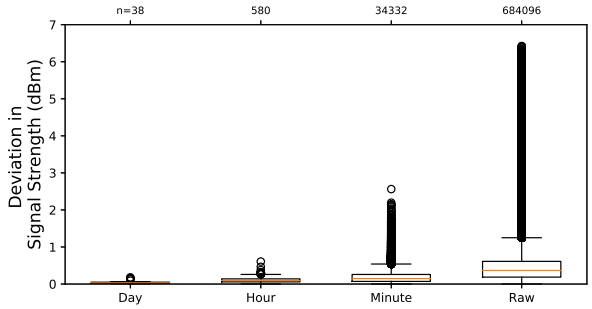

Fig. 5: Distribution of deviation from mean signal strength of all monitored LTE frequencies.

a method stating a signal was Fair when the UE labeled it as Poor) all methods had over a 95% accuracy, with the UAS again leading with a 98% accuracy. A notable result was that error was skewed towards under-predicting the received signal strength. Accounting for this bias when estimating UE reception would improve accuracy further.

B. Longitudinal Analysis

From the stationary radio (introduced in Section III-F) we received 684,096 readings over a period of two days. To measure the relative stability of signal strength readings, for each reading we calculated the deviation from the mean of the corresponding frequency. To determine the stability across different time scales, we re-sampled the data over multiple time scales (1 minute, 1 hour, 1 day), averaged the intermediate readings, and re-computed the deviation of each sample. The resulting time-series is shown in Figure 5.

As expected, raw readings (with a sampling frequency of 3 Hz) fluctuated considerably, with a total range of 80dBm and the majority of fluctuations < 7 dBm from the mean. When comparing between minutes the majority of the reading were < 3 dbm from the mean. When comparing hour to hour, the majority of signals deviate < 1 dBm from the mean. Comparing between two days of data, across all frequencies, the majority of signals did not deviate.

We analyzed the distribution of hour to hour signal strengths across the 20 monitored LTE frequencies, as shown in Figure 6. The majority of readings across the two day time span fell within 1 dBm of each other. The largest change of signal strengths between two hours was observed on 739.0 MHz (utilized by AT&T) and 1967.5 MHz (utilized by Verizon) which exhibited 7dBm changes.

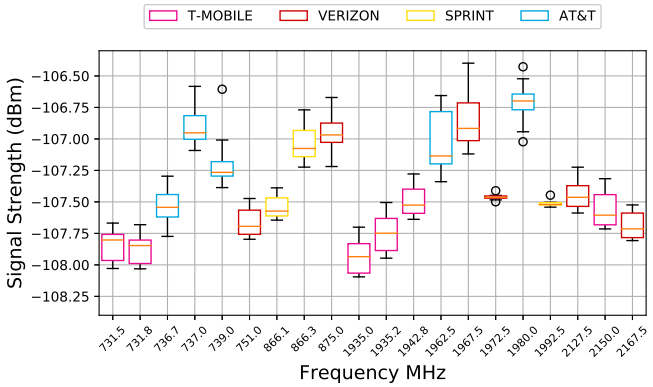

Fig. 6: Distribution of signal strength by frequency over period of observation, averaged across one hour windows.

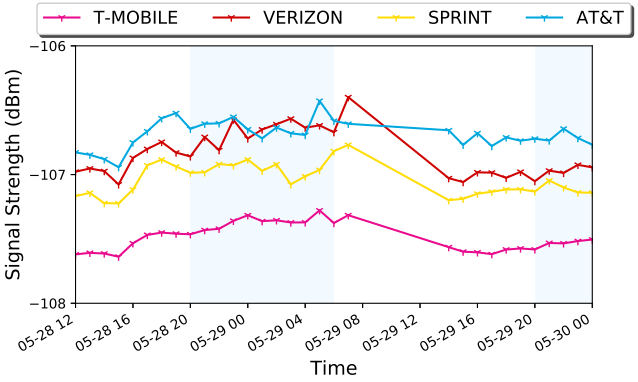

Fig. 7: Signal strength over time by provider gathered by stationary box. Night hours are shaded in blue.

The end user is most impacted by the signal strength of the frequency chosen by the UE. We also examine the hour by hour change of network signal strength. For each operator, for every hour time window, we choose the frequency with the maximum average signal strength. We present the results in Figure 7. While there is a slight improvement in signal strength during night time hours, for each network the total hour to hour fluctuations in signal strength are minimal.

C. Impact of Altitude

To analyze the impact of sampling altitude on signal strength we executed multiple vertical flights in four different locations, as described in Section III-E2. In our analysis, we keep the four locations separated and look at how signal strength at each LTE frequency varies with altitude from the ground. To compare between frequencies, we calculate the deviation of each signal strength measure from the mean of that frequency at each location. We then group altitudes into 20 foot bins and examine the distributions of altitudes across

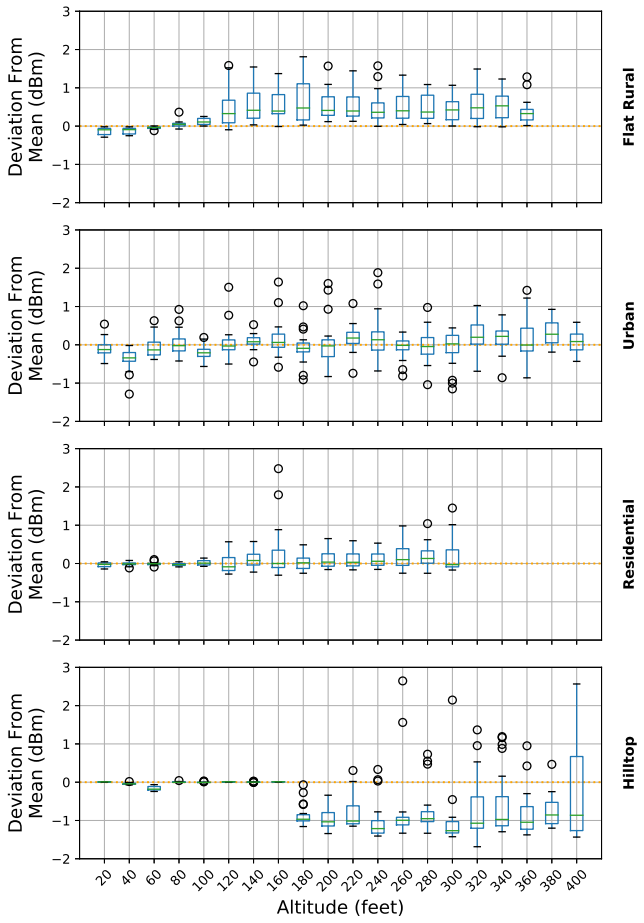

Fig. 8: Deviation of signal strength from mean.

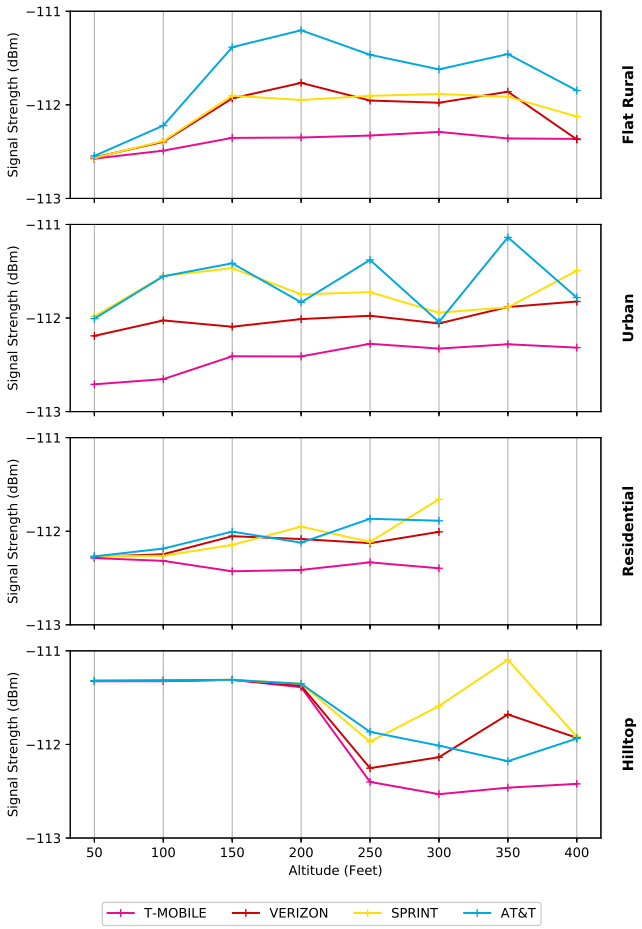

Fig. 9: Signal strength change by altitude and network.

those bins at each of the four locations. We present the results in Figure 8.

Our results show that signal strength variation can be quite dependent on location. The first and third locations, *Flat Rural* and *Residential* respectively, were located level with a wide area of flat terrain surrounded by low hills. At these locations, the vertical UAS flight showed an overall increase in signal strength as altitude increased across LTE frequencies. This might suggest that in low lying terrain, away from strong cellular readings, coverage mapping may be sensitive to flight altitude.

The second location, *Urban*, was located in a more urban area with better cellular coverage. In this area, altitude did not alter the signal strength of frequencies sensed by the UAS. The fourth location, the *Hilltop*, was located high on a hill approximately 400ft above the *Residential* location. At this location, altitudes over 160ft showed a drop in signal strength across most of the monitored LTE frequencies. One possible explanation is that the aerial vehicle may have difficulty detecting coverage at altitudes significantly higher than the provisioned coverage area.

In addition to examining frequency fluctuations, we examine the received signal strength by cellular network provider. In Figure 9 we show the mean change in signal strength across all frequencies with altitude for each network and location. The change is signal is network dependant, and moreover the difference between networks depends on location. A probable explanation for the observed difference is that the eNodeBs serving these networks are in disparate geographic locations, with different signal propagation patterns.

V. Discussion

While we observe clear relationships between sensing methods, the relative signal strength values output by the devices are weakly linearly correlated, particularly to the UEs, even after transforming the data to a common reference frame. We believe the problem stems from difficulty in aligning the various methodologies for comparison. Because we were unable to capture the frequencies on which the UEs operated, we compared the frequencies with the highest signal strength for a given method. This may not always match the actual frequency used by the UE. Additionally, the wardriving readings from the RTL-SDR, USRP, and SA are more difficult to collect due to the labor involved. As a result, there are fewer points of geographic overlap than for the UE and UAS measurements.

By categorizing individual signal strengths by quality, mirroring the "bars" of signal strength that a user's device might report, we were able to accurately match these categorical measurements across measurement methods. As the most versatile collection method, the UAS predicted quality within one gradation over 98% of the time. This aerial signal sensing method demonstrates promise as an effective system for wide-scale cellular coverage mapping.

Based on our experimental data, we generated a coverage map for each method and provider. Figure 10 shows a portion of the map for Verizon. The readings from the UE are shown in Figure 10a and those taken from the UAS on the same day are shown in Figure 10b. Colors and values correspond to Table II, with high RSRP in green and low in red.

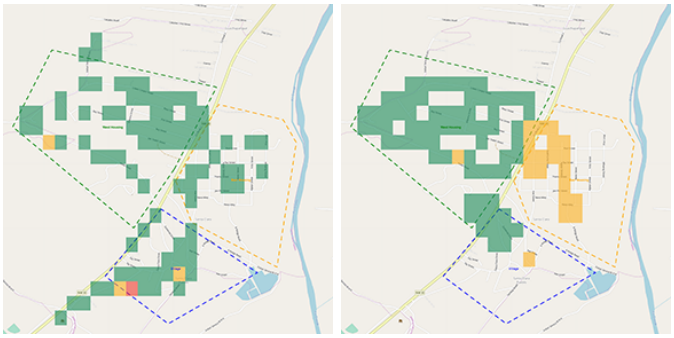

(a) Map from UE readings. (b) Map from UAS readings.

Fig. 10: Cellular coverage map generation.

Next, we evaluated how the design of our aerial data collection impacted the accuracy and precision of UAS signal quality assessment. We considered: 1) how a sample taken at a particular time compares to the overall LTE channel quality during a 24 hour period; and 2) how different UAS altitudes impact this characterization.

Sensing over Time:

Consider the longitudinal analysis of the stationary sensing equipment from Section IV-B. For most frequencies, a single flight *is* sufficient; most readings fell within 3 dBm of each other. However, certain frequencies may be less stable. For example, we found that two channels within the two-day deployment showed values varying by up to 7 dBm, which is wide enough to bump a reading by two signal quality levels (e.g. Good to Fair, or even Poor).

As observed in Figure 6, RTL-SDR signal strength measurements fluctuate between readings. The average of multiple readings provides a more stable description of signal quality in a geographic region. Because the UAS would need to take dozens of samples from a geographic region, the flight pattern and maximum flight speed would vary with the desired granularity of the measurements. The UAS must fly at low speeds to achieve high granularity (e.g. building level accuracy) and higher speeds to achieve greater coverage but lower granularity (e.g. neighborhood level). Alternatively, the UAS can fly at higher speeds following a flight plan that conducts repeated measurements at the same location (e.g. through flight loops).

RF signals sometimes fluctuate based on moisture and other weather conditions. In this study, we did not capture the sensitivity of RTL-SDR signal strength measurements to weather fluctuations and seasonal changes. The stationary sensing equipment was deployed during clear days with no rain, a daily temperature high of $\approx 72°F$ and a low of $\approx 52°F$. In future work, it would be informative to examine how signal readings from an RTL-SDR vary over the course of much longer time spans. Such an assessment could reveal whether the RTL-SDR equipped UAS requires calibration depending on current weather. This type of study would also help with understanding how cellular network quality measurements from our system may fluctuate during or after a natural disaster.

Choice of Altitude:

To measure how altitude affects signal quality, we look to the analysis in Section IV-C. The interaction between altitude and signal strength reception by the UAS is complex. The local geographic topography seems to be the dominant factor in received signal strength. When flying in low valleys, an increase in altitude corresponded to an increase in mean received signal strength. Yet, when ascending from a hilltop above the residential area, signal strength declined. Because the orientation of cellular tower antennas by network providers is provisioned to optimize coverage at elevations of residences and businesses [24], aerial collection at altitudes (in our case approximately five hundred feet above the residential elevation) may see degradation in signal strength.

The effect of altitude on signal quality has implications for evaluating LTE coverage and availability for the occupants of high rise buildings. In dense city centers, we could use aerial systems to map signal strength in three dimensions. Such a measure of signal quality across floors in skyscrapers would not be accounted for by conventional measurement methodologies.

VI. Conclusion

We have shown that a UAS-mounted RTL-SDR is capable of providing a granular reflection of LTE signal strength. Our low-cost solution enables accurate coverage mapping and quality assessment in regions typically neglected by other forms of assessment. Moreover, our system achieves this without requiring expensive specialized equipment, extensive time commitments, or significant manpower. We hope that our work will pave the way for future solutions that more accurately represent cellular coverage, particularly in those regions that are likely under-served.

Acknowledgment

Our work would not have been possible without the incredible support of Jerrold Baca. Thanks to Sherri Conklin for proofreading this manuscript. This work was funded in part through National Science Foundation Smart & Connected Communities award NSF-1831698 and through an NSF Graduate Research Fellowship.

REFERENCES

[1] K. Salemink, D. Strijker, and G. Bosworth, "Rural development in the digital age: A systematic literature review on unequal ICT availability, adoption, and use in rural areas," *Journal of Rural Studies*, vol. 54, pp. 360–371, 2017.

[2] Federal Communications Commission, "Broadband Deployment Report," February 2018. [Online]. Available: https://www.fcc.gov/reports-research/reports/broadband-progress-reports/2018-broadband-deployment-report

[3] Federal Communications Commission., "Connect America Fund (CAF)," February 2017. [Online]. Available: https://www.fcc.gov/general/connect-america-fund-caf

[4] J. E. Prieger, "Mobile data roaming and incentives for investment in rural broadband infrastructure," 2017. [Online]. Available: https://papers.ssrn.com/sol3/papers.cfm?abstract$_id = 3391478$

[5] Federal Communications Commission, "FCC Mobile Broadband Dataset," 2019. [Online]. Available: https://www.fcc.gov/form-477-mobile-voice-and-broadband-coverage-areas

[6] J. Kahan, "It's time for a new approach for mapping broadband data to better serve americans," Apr 2019. [Online]. Available: https://blogs.microsoft.com/on-the-issues/2019/04/08/its-time-for-a-new-approach-for-mapping-broadband-data-to-better-serve-americans/

[7] Rural Wireless Association, "Challenges faced by small wireless providers in measuring LTE coverage," Dec 2018. [Online]. Available: https://ruralwireless.org/rwa-welcomes-fcc-investigation-into-violation-of-mobility-fund-phase-ii-mapping-rules/

[8] Rural Wireless Association., "RWA Calls for FCC Investigation of T-Mobile Coverage Data," 2018. [Online]. Available: https://ruralwireless.org/rwa-calls-for-fcc-investigation-of-t-mobile-coverage-data/

[9] S. Meinrath, H. Bonestroo, G. Bullen, A. Jansen, S. Mansour, C. Mitchell, C. Ritzo, and N. Thieme, "Broadband availability and access in rural pennsylvania," June 2019. [Online]. Available: https://www.rural.palegislature.us/broadband/Broadband_Availability_and_Access_in_Rural_Pennsylvania_2019_Report.pdf

[10] Measurement Lab, "Open Internet Measurement." [Online]. Available: https://www.measurementlab.net

[11] Government Accountability Office, "Broadband Internet: FCC's Data Overstate Access on Tribal Lands," September 2018.

[12] FCC, "Understanding wireless telephone coverage." [Online]. Available: https://fcc.gov/consumers/guides/understanding-wireless-telephone-coverage-areas

[13] CellMapper. [Online]. Available: https://www.cellmapper.net

[14] OpenSignal. [Online]. Available: https://www.opensignal.com/

[15] C. Hurley, R. Rogers, F. Thornton, and B. Baker, *Wardriving and Wireless Penetration Testing*. Syngress, 2007.

[16] M. C. Batistatos, G. E. Athanasiadou, D. A. Zarbouti, G. V. Tsoulos, and N. C. Sagias, "LTE ground-to-air measurements for UAV-assisted cellular networks," in *12th European Conference on Antennas and Propagation (EuCAP)*. IET, 2018.

[17] G. E. Athanasiadou, M. C. Batistatos, D. A. Zarbouti, and G. V. Tsoulos, "LTE ground-to-air field measurements in the context of flying relays," *Wireless Communications*, vol. 26, no. 1, pp. 12–17, 2019.

[18] C. Desmond, "Verizon Uses Drones During Disasters like Hurricane Harvey," Nov 2017. [Online]. Available: https://www.roboticstomorrow.com/article/2017/11/article/11068

[19] M. Nekrasov, R. Allen, and E. Belding, "Performance Analysis of Aerial Data Collection from Outdoor IoT Sensor Networks using 2.4 GHz 802.15.4," in *Proceedings of the 5th Workshop on Micro Aerial Vehicle Networks, Systems, and Applications*. ACM, 2019.

[20] M. Nekrasov, R. Allen, I. Artamonova, and E. Belding, "Optimizing 802.15.4 Outdoor IoT Sensor Networks for Aerial Data Collection," *Sensors*, vol. 19, no. 16, 2019.

[21] Osmocom, "RTL-SDR." [Online]. Available: https://osmocom.org/projects/rtl-sdr/wiki/Rtl-sdr

[22] F. Minucci, S. Rajendran, B. V. d. Bergh, S. Pollin, D. Giustiniano, H. Cordobés, R. C.-P. Fuchs, V. Lenders *et al.*, "Electrosense-spectrum sensing with increased frequency range," in *Proceedings of the 2018 International Conference on Embedded Wireless Systems and Networks*. Junction Publishing, 2018.

[23] J. A. del Peral-Rosado, J. M. Parro-Jiménez, J. A. López-Salcedo, G. Seco-Granados, P. Crosta, F. Zanier, and M. Crisci, "Comparative results analysis on positioning with real LTE signals and low-cost hardware platforms," in *7th ESA Workshop on Satellite Navigation Technologies and European Workshop on GNSS Signals and Signal Processing (NAVITEC)*. IEEE, 2014.

[24] X. Lin, R. Wiren, S. Euler, A. Sadam, H.-L. Maattanen, S. D. Muruganathan, S. Gao, Y.-P. E. Wang, J. Kauppi, Z. Zou, and V. Yajnanarayana, "Mobile networks connected drones: Field trials, simulations, and design insights," *arXiv*, 2018.

[25] O. Genc, M. Bayrak, and E. Yaldiz, "Analysis of the Effects of GSM Bands to the Electromagnetic Pollution in the RF Spectrum," *Progress In Electromagnetics Research*, vol. 101, 2010.

[26] S.-K. Noh and D. Choi, "Propagation Model in Indoor and Outdoor for the LTE Communications," *International Journal of Antennas and Propagation*, 2019.

[27] K. Shamaei, J. Khalife, and Z. M. Kassas, "Exploiting LTE signals for navigation: Theory to implementation," *Transactions on Wireless Communications*, vol. 17, no. 4, pp. 2173–2189, 2018.

[28] A. Saeed, K. A. Harras, E. Zegura, and M. Ammar, "Local and low-cost white space detection," in *37th International Conference on Distributed Computing Systems (ICDCS)*, June 2017.

[29] O. Simpson and Y. Sun, "LTE RSRP, RSRQ, RSSNR and local topography profile data for RF propagation planning and network optimization in an urban propagation environment," *Data in brief*, vol. 21, pp. 1724–1737, 2018.

[30] C. Lin, K. Sandrasegaran, H. A. M. Ramli, and R. Basukala, "Optimized performance evaluation of LTE hard handover algorithm with average RSRP constraint," *CoRR*, vol. abs/1105.0234, 2011. [Online]. Available: http://arxiv.org/abs/1105.0234

[31] K. Dimou, M. Wang, Y. Yang, M. Kazmi, A. Larmo, J. Pettersson, W. Muller, and Y. Timner, "Handover within 3GPP LTE: Design Principles and Performance," in *70th Vehicular Tech. Conf.* IEEE, 2009.

[32] P. Legg, G. Hui, and J. Johansson, "A Simulation Study of LTE Intra-frequency Handover Performance," in *72nd Vehicular Tech. Conf.* IEEE, 2010.

[33] D. Aziz and R. Sigle, "Improvement of LTE Handover Performance through Interference Coordination," in *69th Vehicular Tech. Conf.* IEEE, 2009.

[34] J. Kurjenniemi, T. Henttonen, and J. Kaikkonen, "Suitability of RSRQ measurement for quality based inter-frequency handover in LTE," in *Intern. Symposium on Wireless Communication Sys.* IEEE, 2008.

[35] M. Anas, F. D. Calabrese, P. E. Mogensen, C. Rosa, and K. I. Pedersen, "Performance evaluation of received signal strength based hard handover for UTRAN LTE," in *65th Vehicular Tech. Conf.* IEEE, 2007.

[36] J. Kurjenniemi and T. Henttonen, "Effect of measurement bandwidth to the accuracy of inter-frequency RSRP measurements in LTE," in *19th International Symposium on Personal, Indoor and Mobile Radio Communications*. IEEE, 2008.

[37] F. Afroz, R. Subramanian, R. Heidary, K. Sandrasegaran, and S. Ahmed, "SINR, RSRP, RSSI and RSRQ measurements in long term evolution networks," *International Journal of Wireless & Mobile Networks*, 2015.

[38] C. Ide, B. Dusza, and C. Wietfeld, "Performance of channel-aware M2M communications based on LTE network measurements," in *24th Annual International Symposium on Personal, Indoor, and Mobile Radio Communications (PIMRC)*. IEEE, 2013.

[39] C. Ide, R. Falkenberg, D. Kaulbars, and C. Wietfeld, "Empirical analysis of the impact of LTE downlink channel indicators on the uplink connectivity," in *83rd Vehicular Tech. Conf.* IEEE, 2016.

[40] C. S. Park and S. Park, "Analysis of RSRP measurement accuracy," *Communications Letters*, vol. 20, no. 3, pp. 430–433, 2016.

[41] H. C. Nguyen, R. Amorim, J. Wigard, I. Z. Kovacs, and P. Mogensen, "Using LTE networks for UAV command and control link: A rural-area coverage analysis," in *86th Vehicular Tech. Conf.* IEEE, 2017.

[42] R. Amorim, H. Nguyen, P. Mogensen, I. Z. Kovács, J. Wigard, and T. B. Sørensen, "Radio channel modeling for UAV communication over cellular networks," *Wireless Communications Letters*, vol. 6, no. 4, pp. 514–517, 2017.

[43] B. Lubek, "Network monitor." [Online]. Available: https://github.com/caarmen/network-monitor

[44] Taoglas, "Apex III Wideband 4G LTE Dipole Terminal Antenna," 2019. [Online]. Available: https://cdn3.taoglas.com/datasheets/TG.45.8113.pdf

[45] srsLTE. [Online]. Available: https://github.com/srsLTE/srsLTE

[46] SignalBooster, "What is strong signal in dBm for 4G?" April 2016. [Online]. Available: https://www.signalbooster.com/blogs/news/differences-between-3g-1x-vs-4g-lte-signal-strength-in-dbm